

RESEARCH ARTICLE

Catalyst degradation under different test and poisoning conditions – Comparison parameters definition to map the effects on proton exchange membrane fuel cell voltage

Eleonora Gadducci  | Tommaso Reboli | Massimo Rivarolo | Loredana Magistri

Thermochemical Power Group,
Università degli Studi di Genova – DIME,
Genova, Italy

Correspondence

Eleonora Gadducci, Università degli Studi
di Genova – DIME. Via Montallegro 1,
16145 Genova, Italy.
Email: eleonora.gadducci@edu.unige.it

Abstract

Proton exchange membrane fuel cells (PEMFCs) are considered among the most promising technologies for hydrogen utilization in both stationary and transport applications. Nevertheless, the cost of its components – especially the catalyst and the membrane – is still consistent and far from the cost predicted by the US Department of Energy. It is therefore essential to predict the effect of contaminants on PEMFC materials and to estimate their useful life. The literature on this topic is consistent, but the absence of standards for the experimental tests under contaminated flows makes it difficult to extrapolate the generic degradation trends and compare the results of different publications. This work aims to collect and interpret the results of the recent studies on catalyst contamination: the voltage degradation rate and reduction effect are defined via a data modeling work to understand and compare the effects of different contaminants, their concentrations, exposure times, and current densities. Thanks to the results of the present study, some conclusions are drawn regarding the impact of the different pollutants on cell voltage decay, with attention dedicated to establishing a correlation that takes into account also the different operating conditions.

KEYWORDS

hydrogen, PEM fuel cells, catalyst, degradation, contaminants

1 | INTRODUCTION

Global concerns about climate change are pushing toward a new and more sustainable energy production system. Emissions should be lowered, and renewables play an important role in the production phase, while batteries and hydrogen are interesting as energy storage and energy vec-

tors. Therefore, hydrogen and fuel cells (FCs) are acquiring increasing attention. The price of the technology is still high, while the US Department of Energy (DoE) targeted a strong reduction of the FCs production cost during the last years. The latter was supposed to approach 40\$ kW⁻¹ in 2017 [1–4]. This target was not fully reached: the cost was in fact around 45\$ kW⁻¹ in 2017 for automotive systems. The research by Whiston et al. [4] compared, in 2019, the experts' opinions about the proton exchange membrane fuel cell (PEMFC) system's cost with DoE target and estimations. The study shows a good agreement between DoE cost targets and experts' estimations in the long term (2050).

List of Abbreviations: AST, accelerated stress test; CL, catalyst layer; DoE, Department of Energy; ECA, emission control areas; FC, fuel cell; FCEV, fuel cell electric vehicle; HOR, hydrogen oxidation reaction; LLT, long-lasting test; ORR, oxygen reduction reaction; PEMFC, proton exchange membrane fuel cell; RE, reduction effect.

FC systems are thus becoming cost-competitive with traditional internal combustion engines; they as well ensure a high energy density, high efficiency, no greenhouse gas emissions during operation, and the possibility of scaling up the system size through their modularity. Hydrogen's potential is nowadays exploited in domestic, stationary, and automotive applications [5, 6], for both heat and electricity [7, 8]. In the automotive field, PEMFCs are considered the most promising low-emission technology, thanks to the low operating temperatures which allow fast starts and stops and load changes. New PEMFC installations are under experimentation for light-duty vehicles, heavy-duty vehicles, and trains. Based on the International Energy Agency report on fuel cell electric vehicles (FCEV), there is an estimation of 17% FCEV share in the market by 2050 [9]. Recent production increases have been announced by different automotive manufacturers, such as Toyota [10] and Hyundai [11], and by fuel cell stack producers (Symbio plans to produce 200,000 fuel cell stacks per year [12]), to reach over 3.7 million FCEV equivalents per year by 2030 [13].

Indeed, PEMFCs show many advantages also with respect to battery electric vehicles including lower weight and charging time, prolonged driving autonomy, and less environmental side effects. As regards ships, the emission regulations have become stricter in recent years, especially for what concerns Particulate Matter, SO_x – whose content limit in terms of weight in the fuel has been lowered from 3.5% to 0.5% in 2020, with further limitation to 0.1% in emission control areas (ECA) – and NO_x – whose emissions must comply with the Tier III limit (on NO_x emissions) in ECA [14–16]. These limitations are no longer achievable with traditional engines and fuels [17], also considering the long-term targets set by the International Maritime Organization [18]. Since PEMFC systems can ensure emissions reduction, extended operative ranges [19–21], and low noise and vibrations [22], different feasibility studies have been developed in recent times [23–28], considering their behavior in different hydrogen storage technologies, environmental and dynamic conditions [29–34] as well as in hybrid configurations [35–38].

However, some of the components of PEMFCs are very sensitive to environmental and operating conditions. New research is assessing the potential of innovative materials for the catalyst layer (CL), for an instance, to improve durability and reduce the cost [39–41]. Nevertheless, many studies have demonstrated that the current catalyst technology can be poisoned by external contaminants – present in the hydrogen is produced from fossil resources, and in the air, if it is taken from polluted areas such as traffic urban areas or engine rooms – which then enter in the fuel cell through the anode and/or the cathode

inlets [30–33, 35–53]. If catalyst degradation is verified, the achievable cell voltage can decrease permanently, causing a significant performance loss. This work has the scope of reviewing the research and State of Art on catalyst degradation by poisoning, and its effects on the cell voltage. Once the literature results are collected, they will be analyzed and compared, aiming to define an analytical tool to predict cell voltage degradation depending on the operative and environmental conditions.

2 | SCIENTIFIC APPROACH

The CL – meant as the globality of sites of electrochemical reaction – is a vital part of the PEMFCs that plays an important role in their durability. Platinum nanoparticles on black carbon (Pt/C) are widely employed as a catalyst in low-temperature PEMFC's anodes and cathodes. This is because Pt is the most active noble metal, and it has a good efficiency at relatively low temperatures for both hydrogen oxidation reactions (HORs) at the anode and oxygen reduction reactions (ORRs) at the cathode. However, Pt is expensive and rare and it can be easily poisoned by a range of impurities and contaminants present both in hydrogen and air: contaminants occupy the active sites of the catalyst, which therefore loses its ability to enhance the HOR and ORR.

Hydrogen quality must be high and compliant with different international standards: thirteen gaseous contaminants must be monitored according to ISO 14687:2019 [54] (Table 1), SAE J2719:2020 [55], and EN 17124:2019 [56]. The common substances that are most dangerous to the catalyst at the anode side are carbon monoxide (limit: 0.2 ppmv), sulfur compounds (limit: 0.004 ppmv), ammonia (limit: 0.1 ppmv), nitrogen compounds, and hydrocarbons in general (total limit: 100 ppmv) [42, 57]. The most detrimental pollutant that may reach the CL through the cathode side is in general the air contaminants (the ones found in traffic urban areas such as particulate, naphthalene, acetylene, and ozone) as well as carbon, nitrogen, and sulfur oxides [43, 58–63]. According to the United States Environmental Protection Agency, nitrogen and sulfur dioxide present in the air have been following a decreasing trend during the last 40 years, with an average concentration nowadays respectively between 0.050–0.035 and 0.035–0.010 ppm [64]. As regards sulfur dioxide, its average concentration in the air could already be detrimental to the CL, considering the related restrictions applied to the hydrogen gas. Yet, some concentration peaks can be verified in traffic areas, also depending on the environmental conditions (wind speed, precipitations). This is particularly relevant for other pollutants, such as

TABLE 1 Hydrogen fuel impurities limitations for PEMFC use, ISO 14687-2 [54]

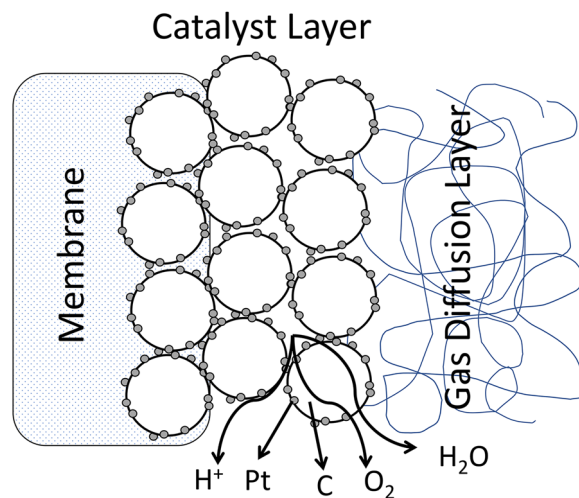
Component	Chemical Formula	Limit	Unit
Hydrogen, min	H ₂	99.97	%
Total non-hydrogen		300	ppmv
Argon	Ar	100	ppmv
Carbon dioxide	CO ₂	2	ppmv
Carbon monoxide	CO	0.2	ppmv
Helium	He	300	ppmv
Formic acid	HCOOH	0.2	ppmv
Formaldehyde	HCHO	0.01	ppmv
Ammonia	NH ₃	0.1	ppmv
Nitrogen	N ₂	100	ppmv
Oxygen	O ₂	5	ppmv
Water	H ₂ O	5	ppmv
Particulates		0.001	g kg ⁻¹
Total sulfur	H ₂ S, COS, CS ₂ , etc.	0.004	ppmv
Total halogenated compounds		0.05	ppmv
Total hydrocarbon content ex. methane		2	ppmv
Total methane nitrogen and argon	CH ₄ , N ₂ , Ar	100	ppmv

carbon monoxide, which can reach a concentration of up to 3.1 ppm in traffic areas during rush hours [65], while its content limit in hydrogen gas is set at 0.2 ppm.

Since the main component of the CL is the same, the most dangerous poisoning components are similar at the two cell sides. Moreover, the air contaminants may also permeate through the membrane and reach the anode's catalyst, increasing the effects of chemical degradation due to contamination and partially nullifying the strict regulations on hydrogen quality. Ionic substances – such as chlorine – should be avoided in the reactants flows, too. However, they are usually more detrimental to the polymeric membrane, as they tend to create bonds with the end part of the membrane's acidic chains and are therefore not deepened in this study.

While hydrogen quality is accurately monitored before the use in PEMFCs, on the other hand, it is more difficult to control the quality of air entering the cathode, considering that it strongly depends on the application and the context (i.e., vehicles, shipping, and stationary applications). This results in no standard definition of air quality for PEMFCs.

Many scientific reports have studied the effect of specific contaminant species on the degradation of the catalyst, but poisoning studies mostly consider just one species at a time. Also, the effect of contamination coupled with

**FIGURE 1** Schematic diagram of Pt/C catalyst structure

dynamic operating conditions is yet poorly investigated in the literature, while it is relevant: contaminants show different effects depending on operating temperature, pressure, potential, exposure time, contaminant concentration, etc. This confirms that research is still needed to make assumptions closer to reality. Finally, contamination studies in literature never follow a testing protocol. This increases the difficulty of defining a trend in the effect of a specific poisoning compound and of comparing it to others.

2.1 | Catalyst contamination mechanisms

The description of contamination mechanisms in the present Section is linked to the chemical ones on the CL, as this is the core of the study. As previously described, the catalyst in PEMFC is a platinum-based material embedded in a porous conductive substance – usually carbon black powder – that acts as a catalyst support layer (Figure 1). It is disposed on the membrane in the form of small-sized particles, to achieve the maximum electrochemically active area. The amount of Pt in a single cell is usually around 40 mg cm⁻². This amount is foreseen to be reduced to decrease the cost of PEMFC technology. However, it is crucial to understand the mechanisms behind and thus limit the degradation of such an expensive component and maximize its useful life. Due to its high chemical activity, platinum can be affected by the presence of impurities in the reactants streams (hydrogen and oxygen/air). This condition can lead to a direct decrease in the electrochemically active surface area as the Pt active sites are occupied by molecules of contaminants. Platinum can in fact easily react, for instance, with the most common substances

found in hydrogen when obtained from hydrocarbons processing (CO, CO₂, N₂, SO₂, H₂S, NH₃, etc.) but also with other impurities such as the ones present in traffic urban areas. According to reference [66], the main mechanisms by which contaminants affect the CL are the following: they can dilute the reactant's concentration, increasing diffusive losses; inert gases such as CO₂ can be reduced, in presence of Pt, to more dangerous components and thus affect the CL [67]; they can be adsorbed on the surface of the Pt catalyst, reducing the available active sites for HOR and ORR; they can aggregate into bigger molecules in presence of Pt and irreversibly destroy the catalyst surface activity [68]; they can combine with H⁺ and form ionized compounds, reducing the conductivity of the electrolyte membrane [69].

When contaminants are adsorbed by the CL, the more active sites are occupied by poisoning compounds, and the more PEMFC's performance is affected, as the HOR and ORR are instead hindered. The phenomenon eventually results in a decrease in cell voltage. The consequences can vary depending on the amount of contaminant and on operating conditions; besides, in some cases, consequences can be partially recovered by dedicated procedures, such as a small percentage of O₂ can be injected together with the H₂ to preferentially oxidize CO and partly remove it from the CL at the anode [70–72]; cyclic voltammetry scanning can recover cells performance after H₂S or SO₂ contamination [73, 74]; the injection of pure hydrogen after a poisoning phenomenon can in some cases be sufficient to improve cells performance [75]. However, a residual cell voltage loss is permanent and leads to a reduction in the useful life of PEMFC.

The present work has focused on CL degradation by five contaminants: CO, H₂S, NH₃, NO₂, and SO₂. Results only for single PEMFC cells under stress tests have been considered, and not on the tests concerning multi-cell stacks since the number of cells may vary among the available literature. This choice is intended to obtain a more reliable comparison between results. On the other hand, as contaminants and materials are similar at the anodic and cathodic sides, and considering the membrane permeability to the contaminants, these results have been analyzed together. Accelerated stress tests (ASTs) and long-lasting tests (LLTs) have been considered. The firsts (which involve high contaminant concentrations and short time) are usually more convenient from the economic and time demand side; however, they differ from real operative conditions and can give misleading information. Indeed, platinum poisoning after a certain time tends to reach an equilibrium point, where associative and dissociative reactions with the contaminant are almost even. Thus, the degradation effect results smoothed if observed in the long term. However, both AST and LLT are included in the

present work, with the aim of identifying the shortest time a test should last to obtain consistent results.

To understand the effect of contaminants at different test conditions, a deep literature investigation of experimental results has been carried out. Different articles have been found, which reported the results of experimental activities concerning CL poisoning to affect quantification. The presence of CL degradation can be usually detected by a voltage reduction. Therefore, to estimate the degradation level, it is useful to evaluate the voltage reduction measured at the same current density. For this reason, only the articles containing the evaluation of voltage reduction have been considered for the present work, and the authors which had instead defined a current reduction at a given voltage value, difficult to be compared, have been excluded. A data modeling work has been developed based on selected literature results to define significant original parameters which can help understand the effect of CL poisoning on cell voltage.

2.2 | Calculations

On a first attempt, a percentage voltage decay V_D has been computed for the results found in the literature. This is obtained with Equation (1), comparing the baseline cell voltage defined in the respective publication to the cell voltage measured after the stress test:

$$V_D = 100 \cdot \frac{V_{baseline} - V_{after_test}}{V_{baseline}} \quad (1)$$

where V_D is the percentage voltage decay (%), $V_{baseline}$ is the initial cell voltage (V), and V_{after_test} is the final cell voltage (V).

The voltage decay V_D has been employed at the beginning of this study to analyze results concerning a single contaminant provided to the PEMFC at a constant concentration and to check the influence of exposure time and current density on CL degradation. However, the V_D value resulted in very different and non-comparable results that are obtained at different exposure times, neither within tests that employ the same contaminant.

To make AST and LLT results comparable, a new average voltage decay rate V_{DR_avg} has been defined from the voltage decay V_D divided by the exposure time. V_{DR_avg} is calculated via Equation (2):

$$V_{DR_avg} = \frac{V_D}{\Delta t} \quad (2)$$

where V_{DR_avg} is the average voltage decay rate (% h⁻¹), V_D is the percentage voltage decay (%), and Δt is the test duration (h).

This value can be used as a reference to compare the results of studies at different durations available in the literature. However, if an AST is implemented for a time shorter than 1 h, the V_D value can be misleading resulting in values higher than 100%. These values are not consistent, but it is due to the voltage decrease that can be very strong in the first minutes of exposure to the contaminant due to the kinetics of the reactions affecting the CL. This fact underlines the necessity of longer stress tests. The V_{DR_avg} has been calculated for all the results found in the literature, allowing a general comparison among the 5 contaminants and their effect on cell voltage.

Nevertheless, the V_D and V_{DR_avg} obtained did not allow the definition of a trend to describe the degradation effect at different contaminants concentrations, exposure times, and current density. To have a more global view of the CL degradation phenomenon, and to account for more than one factor at the same time, it has been necessary to define new parameters. The first one is the Coulomb density (C_D), and it is obtained through Equation (3). The Coulomb density allows us to consider both the current density at which the experimental test is developed and the test duration:

$$C_D = I_D \cdot \frac{\Delta t}{3600} \quad (3)$$

where C_D is the Coulomb density ($C \text{ cm}^{-2}$), I_D is the current density ($A \text{ cm}^{-2}$), and Δt is the test duration (h).

The final parameter defined in this work has been named reduction effect (RE). This is an indicator of the contaminant mass that reaches the fuel cell, and it is obtained by Equation (4):

$$RE = C_D \cdot C_{conc} \quad (4)$$

where RE is measured as $C \text{ ppm cm}^{-2}$, C_D is the Coulomb density ($C \text{ cm}^{-2}$), and C_{conc} is the contaminant concentration (ppm).

The RE can quantify the degradation of the CL in terms of V_{DR_avg} depending on the operative conditions (concentration, time, current density).

3 | RESULTS AND DISCUSSION

Tables 2–6 resume the most interesting results for V_D and V_{DR_avg} calculations, obtained starting from literature values. These values confirm that, for all the five contaminants investigated, there is a link between the intensity of degradation and the current density, and the exposure time.

Publications found in the literature are generally difficult to be compared, as the absence of test protocols

(temperature, duration, contaminant concentration, load profile) does not allow to exclude some of the variables which instead – as visible from the Tables reported in this work – have a strong influence on cell voltage. In the following paragraphs, a detailed analysis of the effect of each contaminant taken into account is reported.

3.1 | CO contamination

Results for CO contaminations shown in Table 2 are mostly obtained with a pollutant concentration higher than the imposed limit indicated in ISO 14687-2 (0.2 ppm) and higher than the peaks that can be registered in traffic urban areas (3.1 ppm). These tests are in general more detrimental at higher current density and longer exposure time, but in the longer duration, the voltage loss seems more significant for operation at a higher current density. This is well visible in Figure 2 (which contains results for CL poisoning with constant exposure to 10 ppm CO), and it is in accordance with the fact that, at higher current density, the reactants flow is increased and so is the amount of contaminant reaching the CL. Moreover, analyzing Figure 2, it can be seen that for exposure time shorter than 2 h, the effect of the current density seems not to be significant. This conclusion should be corroborated and validated through further experimental data analysis. Therefore, even if in the long term the CL kinetics of contamination reaches equilibrium, a higher concentration results in more impact. As shown in Table 2, just in one case it was possible to appreciate the approach of a steady state in the voltage decay [77]. Yet, the results of AST have an impact on both V_D and V_{DR_avg} which can reach a 1 or 2-orders of magnitude difference. In Figure 3, tests with the same duration reported in [79] are compared instead. The CO concentration and current density vary among four different values, respectively. The results confirm once again the influence of increasing current density as well as the one of increasing CO concentration on the percentage voltage decay. Both the parameters are thus relevant and should be considered in the prediction of long-term effects on PEMFC's useful life. However, at low current densities, the different CO concentrations show no significant difference in voltage decay.

3.2 | H₂S contamination

For what concerns hydrogen sulfide (Table 3), literature results have been found only for anode contamination, as H₂S is not usually present in the air stream. Its tested concentration is also always higher than the allowed amount in the hydrogen stream (0.004 ppm). However,

TABLE 2 Degradation associated with carbon monoxide contamination in literature results

Concentration of CO (ppm)	Time (h)	I_D ($A\ cm^{-2}$)	V_D (%)	V_{DR-Avg} ($\% h^{-1}$)	Constant voltage at steady-state (Yes – No)	Time needed to reach the steady-state (h)	Ref.
10	1145	0.4	9.6	0.01	No	–	[76]
10	1000	0.6	42.2	0.04	No	–	[76]
10	2	0.2	2.5	1.23	No	–	[77]
10	2	0.4	2.5	1.3	No	–	[77]
10	2	0.6	2.8	1.4	No	–	[77]
50	1	1.2	23.4	23.4	Yes	0.75	[77]
2	72	0.8	46.7	0.6	No	–	[78]
100	3.3	0.217	66.2	19.9	No	–	[60]
0.1	4.0	0.1	0.8	0.2	No	–	[79]
0.1	4.0	1	5.3	1.3	No	–	[79]
0.1	4.0	1.7	18.9	4.7	No	–	[79]
0.2	4.0	0.1	1.0	0.3	No	–	[79]
0.2	4.0	1	25.4	6.4	No	–	[79]
0.2	4.0	1.7	42.7	10.7	No	–	[79]
0.3	4.0	0.1	2.1	0.5	No	–	[79]
0.3	4.0	1	39.0	9.7	No	–	[79]
0.3	4.0	1.7	52.5	13.1	No	–	[79]
0.4	4.0	0.1	2.9	0.7	No	–	[79]
0.4	4.0	1	42.2	10.6	No	–	[79]
0.4	4.0	1.7	54.4	13.6	No	–	[79]
0.1	4.0	0.1	0.1	0.0	No	–	[79]
0.1	4.0	1	2.2	0.6	No	–	[79]
0.1	4.0	1.7	7.6	1.9	No	–	[79]
0.2	4.0	0.1	0.8	0.2	No	–	[79]
0.2	4.0	1	11.9	3.0	No	–	[79]
0.2	4.0	1.7	34.9	8.7	No	–	[79]
0.3	4.0	0.1	1.1	0.3	No	–	[79]
0.3	4.0	1	27.5	6.9	No	–	[79]
0.3	4.0	1.7	47.6	11.9	No	–	[79]
0.4	4.0	0.1	1.4	0.3	No	–	[79]
0.4	4.0	1	40.4	10.1	No	–	[79]
0.4	4.0	1.7	56.2	14.0	No	–	[79]
0.1	4.0	0.1	0.3	0.1	No	–	[79]
0.1	4.0	1	0.7	0.2	No	–	[79]
0.1	4.0	1.7	1.9	0.5	No	–	[79]
0.2	4.0	0.1	1.0	0.3	No	–	[79]
0.2	4.0	1	2.6	0.7	No	–	[79]
0.2	4.0	1.7	10.0	2.5	No	–	[79]
0.3	4.0	0.1	1.0	0.3	No	–	[79]
0.3	4.0	1	4.9	1.2	No	–	[79]
0.3	4.0	1.7	26.7	6.7	No	–	[79]
0.4	4.0	0.1	1.6	0.4	No	–	[79]
0.4	4.0	1	14.0	3.5	No	–	[79]
0.4	4.0	1.7	43.5	10.9	No	–	[79]

(Continues)

TABLE 2 (Continued)

Concentration of CO (ppm)	Time (h)	I_D ($A\ cm^{-2}$)	V_D (%)	V_{DR-Avg} ($\%\ h^{-1}$)	Constant voltage at steady-state (Yes – No)	Time needed to reach the steady-state (h)	Ref.
0.1	4.0	0.1	1.1	0.3	No	–	[79]
0.1	4.0	1	0.3	0.1	No	–	[79]
0.1	4.0	1.7	0.2	0.0	No	–	[79]
0.2	4.0	0.1	0.9	0.2	No	–	[79]
0.2	4.0	1	1.6	0.4	No	–	[79]
0.2	4.0	1.7	2.1	0.5	No	–	[79]
0.3	4.0	0.1	1.1	0.3	No	–	[79]
0.3	4.0	1	2.6	0.7	No	–	[79]
0.3	4.0	1.7	4.3	1.1	No	–	[79]
0.4	4.0	0.1	1.0	0.3	No	–	[79]
0.4	4.0	1	4.4	1.1	No	–	[79]
0.4	4.0	1.7	11.1	2.8	No	–	[79]

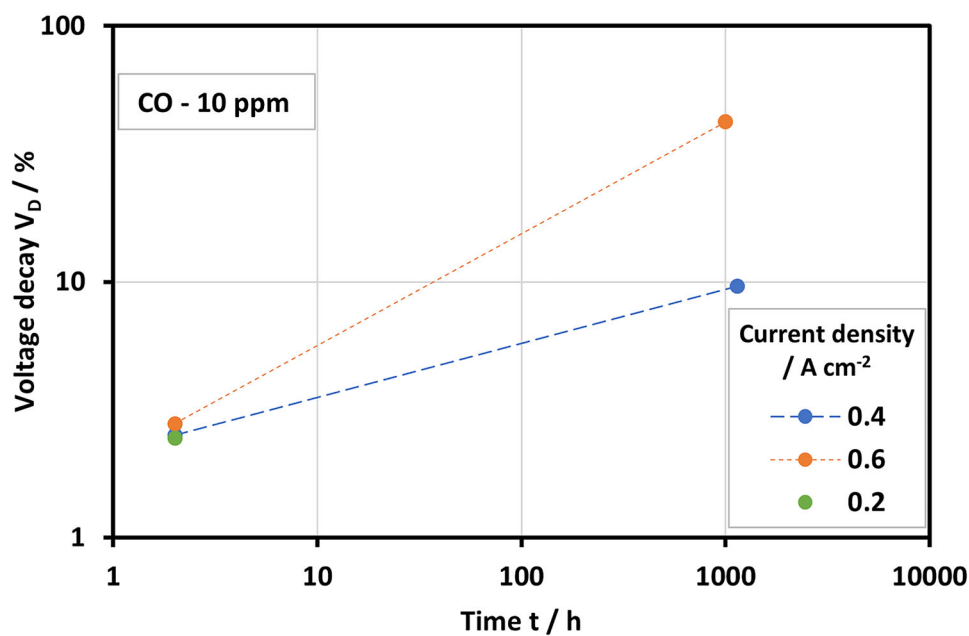
FIGURE 2 V_D for constant (10 ppm) CO contamination at different current densities and exposure time

TABLE 3 Degradation associated with hydrogen sulfide contamination in literature results

Concentration of H_2S (ppm)	Time (h)	I_D ($A\ cm^{-2}$)	V_D (%)	V_{DR-Avg} ($\%\ h^{-1}$)	Constant voltage at steady-state (Yes – No)	Time needed to reach the steady-state (h)	Ref.
1.15	25	0.1	37.2	1.5	Yes	25	[80]
1.95	15	0.5	66.7	4.4	Yes	16	[80]
14.2	3.6	0.5	76.8	21.3	No	–	[80]
11.73	15	0.1	48.2	3.2	No	–	[80]
18	2	0.6	32.0	16.0	No	–	[81]
30	1	0.6	66.0	66.0	No	–	[81]

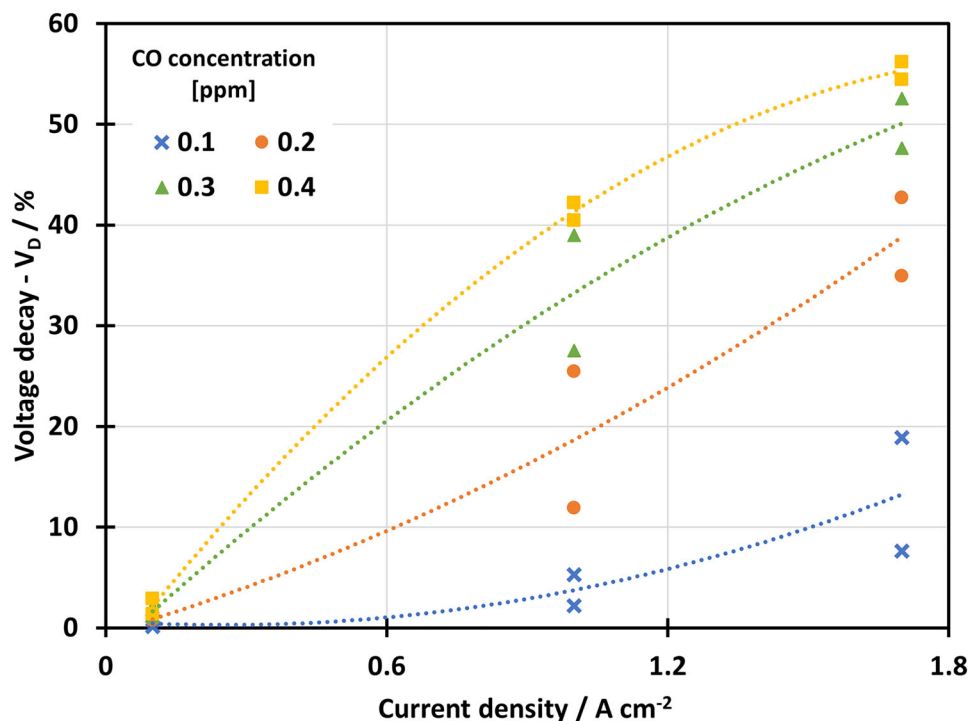


FIGURE 3 V_D for different CO contamination at different current densities and constant (4 h) exposure time

results from the evidence that it causes a higher voltage decay than CO at similar exposure time and concentration (see tests at 18 and 30 ppm of H_2S compared with the results of 50 ppm CO). Nevertheless, results for LLT are lacking in the literature and it is therefore impossible to make a comparison to other contaminants at longer exposure times. It is possible to observe the voltage decay reaching a steady state after less than 30 h of exposure to the contaminant [80]. Nevertheless, other results do not show the same stabilization. Observing the results [80, 89], it can be concluded that the effect of current density is not negligible, and a higher current density has a more detrimental effect. This result is in accordance with the one obtained for the CO contamination case.

3.3 | NH_3 contamination

Contamination by ammonia can be a relevant issue in the medium-long term perspective of using it to store hydrogen. Its limit is set at 0.1 ppm in the hydrogen gas and the experimental results in literature regard tests with higher contaminant concentration (Table 4), provided both at the anode [82] and the cathode side [53, 83]. It causes a voltage decay that is on average in between the one caused by CO and the one caused by H_2S poisoning, and the effect is enhanced at higher current density tests, in agreement with previous results for CO and H_2S contamination effect.

None of the results found in the literature show that voltage decay reaches a steady state after a given exposure time to the contaminant.

3.4 | NO_2 contamination

The NO_2 contamination results found in the literature (Table 5) show a contaminant concentration lower than the limits for total nitrogen compounds in the hydrogen flow (100 ppm) and higher than the one found in urban areas (below 0.05 ppm). While reference [83] analyzes the effects of nitrogen dioxide supplied at the anode, references [84–86] face cathode contamination by air impurities. Short tests indicate that NO_2 exposure can cause a higher voltage decay than CO and NH_3 , but the effect still seems lower than the one caused by H_2S if the 1-h tests at 10 ppm concentration are compared. However, comparing these results can lead to wrong considerations, as the test conditions for NO_2 Contamination are different than for the other contaminants. Indeed, recent literature [66] underlines that generally, sulfur compounds are more harmful than nitrogen compounds. Besides, other results available in the literature assess that NO_2 exposure will cause the voltage decay to reach a steady state, after a first performance drop [90]. Nevertheless, these results could not be employed for the present analysis due to the configuration of data, reported in terms of current decay.

TABLE 4 Degradation associated with ammonia contamination in literature results

Concentration of NH ₃ (ppm)	Time(h)	I _D (A cm ⁻²)	V _D (%)	V _{DR-Avg} (% h ⁻¹)	Constant voltage at steady-state (Yes – No)	Time needed to reach the steady-state (h)	Ref.
200	3.00	0.1	65.1	11.6	No	–	[82]
12.5	48.00	0.5	79.7	0.4	No	–	[82]
25	24.00	0.5	81.1	0.8	No	–	[82]
50	12.00	0.5	75.3	2.1	No	–	[82]
100	6.70	0.5	65.5	5.1	No	–	[82]
200	3.60	0.5	62.2	10.5	No	–	[82]
1	330	1	6.0	0.02	No	–	[53]
1	330	0.75	5.0	0.02	No	–	[53]
1	330	0.5	4.1	0.01	No	–	[53]
2	330	1	5.0	0.02	No	–	[53]
10	1	0.7	10.0	10.00	No	–	[83]

TABLE 5 Degradation associated with nitrogen dioxide contamination in literature results

Concentration of NO ₂ (ppm)	Time (h)	I _D (A cm ⁻²)	V _D (%)	V _{DR-Avg} (% h ⁻¹)	Constant voltage at steady-state (Yes – No)	Time needed to reach the steady-state (h)	Ref.
1	100	0.5	10.45	0.104	No	–	[84]
2.5	24	0.6	7.97	0.332	No	–	[85]
5	12	0.6	12.31	1.026	No	–	[85]
10	1	0.7	20.00	20.000	No	–	[83]
2	31	1	12.43	0.401	No	–	[86]
2	38	0.8	21.09	0.555	No	–	[86]

TABLE 6 Degradation associated with sulfur dioxide contamination in literature results

Concentration of SO ₂ (ppm)	Time (h)	I _D (A cm ⁻²)	V _D (%)	V _{DR-Avg} (% h ⁻¹)	Constant voltage at steady-state (Yes – No)	Time needed to reach the steady-state (h)	Ref.
1	50	0.6	27.82	0.556	Yes	80	[87]
1	100	0.5	35.29	0.353	Yes	60	[84]
2.5	46	0.6	18.84	0.410	No	–	[85]
5	23	0.6	28.26	1.229	No	–	[85]
2	61	0.2	32.00	0.525	Yes	25	[49]
2	59	0.8	53.91	0.914	Yes	20	[49]
2	30	0.6	37.83	1.261	Yes	18	[47]
2	30	0.6	33.87	1.129	Yes	12	[47]
1	60	0.6	37.17	0.620	Yes	18	[88]

3.5 | SO₂ contamination

As regards sulfur dioxide contamination, all the references for this case are dealing with cathode exposure to the poi-

soning compound (Table 6). All the examples found in the literature are comparable in terms of contaminant concentration, exposure time, and current density, and the results evidence that contaminant concentration is not directly

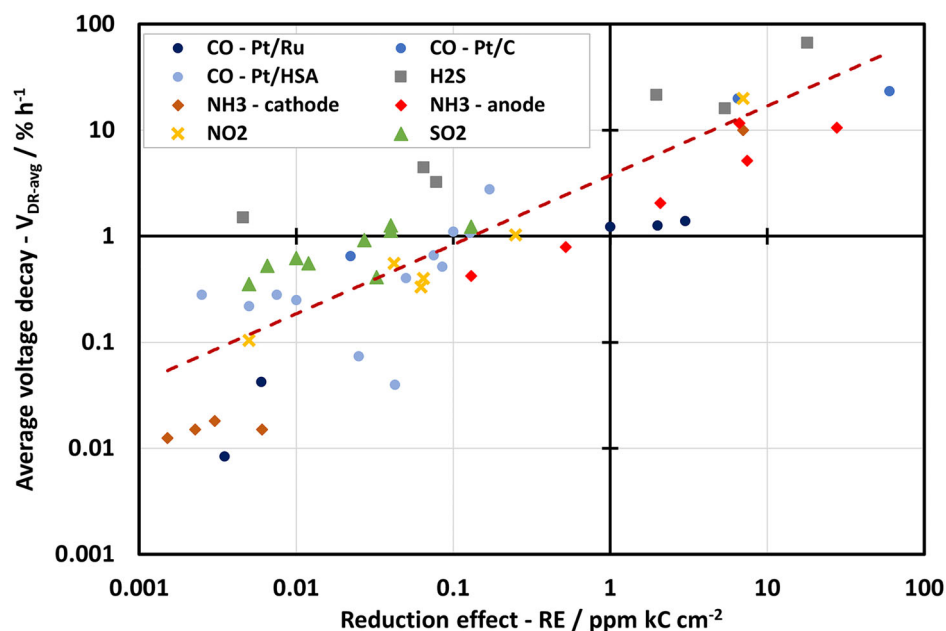


FIGURE 4 Trend of the V_{DR_avg} depending on RE for the literature results investigated

linked to the voltage degradation: indeed, the voltage decay is lower for the 46-h test with 2.5 ppm SO_2 in the supplied air [85] than for the test with 1 ppm developed for 50 h [87]. This happens despite the similar current density implemented during the tests (0.6 A cm^{-2}). Therefore, there may be other parameters that influence the voltage decay which has not been included in the present analysis – such as operative temperature and relative humidity. This topic needs further development in future studies. Except for reference [85], all the other results from the literature assess that the voltage decay reaches a steady state. However, the time needed varies significantly, from a minimum of 12 to a maximum of 80 h. As a general comment, the steady state is reached in a shorter time when the contaminant concentration is higher.

3.6 | Mapping the voltage degradation due to CL contamination

The results collected in this work for the five contaminant species can be useful to predict their generic consequence on FC voltage for single poisoning species. However, although they are commonly implemented, AST can be misleading, considering that a large amount of contaminant is suddenly released in the reactant flows: this is a condition very unlikely to be verified during real operation, while it affects more strongly the conditions of the CL due to its chemical dynamics.

As regards the degradation prediction of a PEMFC exposed to a contaminated reactant flux, the computation

of the RE can give useful information. RE can consider at the same time all the significative parameters involved in CL contamination and degradation (concentration, time, current density). Thanks to results found in the literature, it has been possible to identify a trend that links RE – which can be computed for real-case as well as laboratory tests – to the parameter V_{DR_avg} .

This result, shown in Figure 4, is consistent with the data available in the literature; it underlines – for all the contaminants investigated in this study – the enhancement of the average voltage decay rate at an increasing RE, with the following relation depicted in Equation (5):

$$V_{DR_avg} = a \cdot RE^b \quad (5)$$

where V_{DR_avg} is the average voltage decay ($\% \text{ h}^{-1}$), RE is the reduction effect (C ppm cm^{-2}), a is equal to 3.75 and b is equal to 0.653.

As indicated by Equation (5) the relationship between the average voltage decay and RE is a potential function (as clear in Figure 4 where both axes are logarithmic). This output is also confirming the results as well described in the literature, defining Sulphur-compounds appear as the most detrimental contaminant to the PEMFC's state of health. As regards CO contamination, three different CL alloys have been included in the study (Pt/Ru, Pt/C, and Pt/HSA). The choice of the material seems to have benefits on the average voltage decay, showing that Pt/Ru and Pt/HSA (studied [79]) could be the best choice for operation with respect to Pt/C. Exposure to ammonia at the anode shows a more detrimental effect than it has at

the cathode. Eventually, nitrogen dioxide shows an effect on the average voltage decay between the one caused by ammonia and the one caused by sulfur compounds, in line with the effects of CO exposure.

Further development will include collecting additional experimental outputs in order to increase the reliability of the relation here presented. Moreover, this analysis approach can be addressed to the single contaminant species.

4 | CONCLUSIONS


The present study deepens the topic of catalyst contamination in PEMFC, considering the consequences on the cell voltage. In fact, among the largest bottlenecks to the spread of PEMFC technology are its useful life and the cost of sensitive components such as the CL. Since the end of life can be moved after with an optimized control strategy, it is crucial to identify the most detrimental contaminants in the reactants and estimate their effects in the long term. Therefore, it is also possible to estimate the actual useful life of PEMFC in a real environment with some residual presence of contaminants in the cathodic flow – due to air contaminants in urban areas or engine rooms – and in the anodic flow – due to some remaining impurities in hydrogen. To this aim, a detailed literature review has been developed: the data relative to voltage degradation due to CL contamination have been collected, compared, and analyzed for five different contaminant species. Cathode and anode impurities effects have been assimilated since contaminants can permeate the polymeric membrane and reach the anode, where the effect is more detrimental due to the oxidizing environment. Different operative conditions have been considered, i.e., contaminant type and concentration, exposure time, and current density. An attempt was made via data modeling of existing references in the literature to predict the effects of contaminants on cell voltage depending on the exposure time and operative conditions.

The first consideration related to the present work regards the contamination test implementation: ASTs have the aim of saving time and economical resources and thus they expose PEMFCs for very short times to contaminants concentrations that are not found in real operative conditions. The results of this type of test, however, can be misleading and can give unreliable information on cell durability in standard operative conditions. According to the experimental results found in the literature, a minimum duration of 50 h is needed in a contamination test to estimate reliable cell durability. Moreover, the contaminant concentration must be coherent with the one that can be verified in the environment for real applications.

The main output of this work is the analysis done on the effect of the single contaminant – in particular for CO which is the one with the most comparable tests in similar conditions.

The ambition of this work, however, was also to find an empirical formula that generalizes the effect of the various operating parameters on voltage decay, regardless of the type of contaminant. To do that, some parameters were introduced namely V_D , V_{DR_avg} , C_D , and RE. Thanks to an empirical correlation based on the data available in the literature, it has been possible to map the effects of contaminants on the cell voltage, V_{DR_avg} , as a function of a unique parameter, RE, which includes information on current density, exposure time and contaminant concentration. In this way, knowing the environmental conditions (contaminants concentration) and the operative conditions (current density) it is possible to predict the average voltage decay that will be verified on the FC over time, and therefore predict its useful life.

ORCID

Eleonora Gadducci  <https://orcid.org/0000-0002-8842-6449>

REFERENCES

1. P. Ahmadi, S. H. Torabi, H. Afsaneh, Y. Sadegheih, H. Ganjehsarabi, M. Ashjaee, *Int. J. Hydrogen Energy* **2020**, *45*, 3595.
2. H. Chen, P. Pei, M. Song, *Appl. Energy* **2015**, *142*, 154.
3. Y. Wang, K. S. Chen, J. Mishler, S. C. Cho, X. C. Adroher, *Appl. Energy* **2011**, *88*, 981.
4. M. M. Whiston, I. L. Azevedo, S. Litster, K. S. Whitefoot, C. Samaras, J. F. Whitacre, *Proc. Natl. Acad. Sci. U S A* **2019**, *116*, 4899.
5. Business Korea can be found on <http://www.businesskorea.co.kr/news/articleView.html?idxno=82547> **2021**.
6. Hyundai News can be found on <https://www.hyundainews.com/en-us/releases/2896> **2019**.
7. M. A. Sheshpoli, S. S. Mousavi Ajarostaghi, M. A. Delavar, *Energy* **2018**, *157*, 353.
8. H. Q. Nguyen, B. Shabani, *Energy Convers Manag* **2020**, *204*, 112328.
9. <https://www.iea.org/reports/hydrogen> **2022**.
10. Toyota Motor Corporation. Toyota moves to expand mass production of fuel cell stacks and hydrogen tanks towards ten-fold increase post-2020. https://global.toyota/en/newsroom/corporate/22647198.html?adid=%0Aag478_mail%26padid=ag478_mail.
11. Hyundai. Hyundai motor group reveals 'FCEV vision 2030. **2018**, <https://www.hyundainews.com/en-us/releases/2668>.
12. Fuelcellworks. Symbio to produce 200,000 fuel cell stackpack. **2019**. <https://fuelcellworks.com/news/hydrogen-mobility-at-the-frankfurt-motor%02show-symbio-to-produce-200000-fuel-cell-stackpack/>, accessed March 25, 2020.
13. Fuel Cell and Hydrogen Joint Undertaking. Hydrogen Roadmap Europe: A Sustainable Pathway for the European Energy

- Transition. **2019**, <https://op.europa.eu/en/publication-detail/-/publication/0817d60d-332f-11e9-8d04-01aa75ed71a1>.
14. T. Tronstad, H. Astrand, G. Haugom, L. Langfeldt. Study on the use of fuel cells in shipping. Study commissioned by European Maritime Safety Agency (EMSA) 2017. www.emsa.europa.eu.
 15. H. Wang, P. Zhou, Z. Wang, *J Mar Sci Appl*, **2017**, *16*, 129.
 16. D. Rutherford, B. Comer. The International Maritime Organization's Initial Greenhouse Gas Strategy 2018. <https://www.theicct.org>.
 17. S. Brynolf, M. Magnusson, E. Fridell, K. Andersson, *Transp. Res. Part D Transp. Environ.* **2013**, *28*.
 18. International Maritime Organization (IMO). <https://www.imo.org/en/MediaCentre/HotTopics/Pages/Reducing-greenhouse-gas-emissions-from-ships.aspx>, accessed September 8, 2021.
 19. A. Boudghene Stambouli, E. Traversa, *Renew Sustain Energy Rev*, **2002**, *6*, 295.
 20. L. van Biert, M. Godjevac, K. Visser, P. V. Aravind, *J Power Sources* **2016**, *327*, 345.
 21. O. Z. Sharaf, M. F. Orhan, *Renew Sustain Energy Rev* **2014**, *32*, 810.
 22. J. J. De-Troya, C. Álvarez, C. Fernández-Garrido, L. Carral, *Int J Hydrogen Energy* **2016**, *41*, 2853.
 23. E. Gadducci, T. Lamberti, D. Bellotti, L. Magistri, A. F. Massardo, *Int J Hydrogen Energy* **2021**, *46*, 24305.
 24. M. Rivarolo, D. Rattazzi, T. Lamberti, L. Magistri, *Int J Hydrogen Energy* **2020**, *45*, 25747.
 25. M. Rivarolo, D. Rattazzi, L. Magistri, *Int J Hydrogen Energy* **2018**, *43*, 23500.
 26. R. T. Madsen, L. E. Klebanoff, S. A. M. Caughlan, J. W. Pratt, T. S. Leach, T. B. Appelgate, S. Z. Kelety, H.-C. Wintervoll, G. P. Haugom, A. T. Y. Teo, S. Ghoshe, *Int J Hydrogen Energy* **2020**, *45*, 25328.
 27. H. Nazir, N. Muthuswamy, C. Louis, S. Jose, J. Prakash, M. E. M. Buan, C. Flox, S. Chavan, X. Shi, P. Kauranen, T. Kallio, G. Maia, K. Tammeveski, N. Lymperopoulos, E. Carcadea, E. Veziroglu, A. Iranzo, A. M. Kannan, *Int J Hydrogen Energy* **2020**, *45*, 28217.
 28. G. Borgogna, E. Speranza, T. Lamberti, A. Nicola Traverso, L. Magistri, E. Gadducci, A. Massardo, P. Olivieri, *E3S Web Conf* **2019**, *113*, 1.
 29. M. Cavo, E. Gadducci, D. Rattazzi, M. Rivarolo, L. Magistri, *Int J Hydrogen Energy* **2021**, *46*, 32630.
 30. X. Li, K. Han, Y. Song, *Int J Hydrogen Energy* **2020**, *45*, 20312.
 31. E. Gadducci, T. Lamberti, L. Magistri, M. Rivarolo, A. Dellacasa, B. Campora, G. Borgogna, A. Lancelli, E. Speranza, A. Voiello, *E3S Web Conf* **2022**, *334*, 04003.
 32. M. Cavo, M. Rivarolo, L. Gini, L. Magistri, *Int J Hydrogen Energy* **2022** <https://doi.org/10.1016/j.ijhydene.2022.07.223>.
 33. E. Gadducci, S. Saccaro, M. Rivarolo, L. Magistri, *E3S Web Conf* **2022**, *334*, 04006.
 34. E. Gadducci, T. Lamberti, M. Rivarolo, L. Magistri, *Int. J. Hydrogen Energy* **2022**, *47*, 22545.
 35. P. Wu, R. Bucknall, *Int J Hydrogen Energy* **2020**, *45*, 3193.
 36. A. M. Bassam, A. B. Phillips, S. R. Turnock, P. A. Wilson, *Int J Hydrogen Energy* **2017**, *42*, 623.
 37. A. Bouakkaz, A. J. G. Mena, S. Haddad, M. L. Ferrari, *J Energy Storage* **2021**, *33*, 101887.
 38. A. Giugno, L. Mantelli, A. Cuneo, A. Traverso, *Appl Energy* **2020**, *279*, 115785.
 39. Y. Guo, F. Pan, W. Chen, Z. Ding, D. Yang, B. Li, P. Ming, C. Zhang, *Springer* **2021**, *4*.
 40. S. Zhang, M. Chen, X. Zhao, J. Cai, W. Yan, J. C. Yen, S. Chen, Y. Yu, J. Zhang, *Electrochem Energy Rev* **2021**, *4*, 336.
 41. Z. Xu, W. Deng, X. Wang, *Springer* **2021**, *4*.
 42. W. Shi, B. Yi, M. Hou, Z. Shao, *Int J Hydrogen Energy* **2007**, *32*, 4412.
 43. U. Misz, A. Talke, A. Heinzl, B. P. Effects, *Fuel Cells* **2018**, *18*, 594.
 44. J. St-Pierre, *Int J Hydrogen Energy* **2011**, *36*, 5527.
 45. Y. Zhao, B. P. Setzler, J. Wang, J. Nash, T. Wang, B. Xu, Yan Y. Joule **2019**, *3*, 2472.
 46. A. Moradi Bilondi, M. Abdollahzadeh, M. J. Kermani, H. Heidary, P. Havaej, *Energy Convers Manag* **2018**, *177*, 519.
 47. Y. Zhai, G. Bender, K. Bethune, R. Rocheleau, *J Power Sources* **2014**, *247*, 40.
 48. T. Reshetenko, V. Laue, U. Krewer, K. Artyushkova, *J Power Sources* **2019**, *438*, 226949.
 49. T. Reshetenko, V. Laue, U. Krewer, K. Artyushkova, *J Power Sources* **2020**, *458*, 228032.
 50. O. Lemaire, B. Barthe, L. Rouillon, A. Franco, *ECS Trans* **2019**, *25*, 1595.
 51. M. Angelo, K. Bethune, R. Rocheleau, *Electrochem Soc* **2019**, *28*, 169.
 52. A. Talke, U. Misz, G. Konrad, A. Heinzl, *J Electr Eng* **2015**, *3*, 70.
 53. X. Z. Yuan, H. Li, Y. Yu, M. Jiang, W. Qian, S. Zhang, H. Wang, S. Wessel, T. T. H. Cheng, *Int J Hydrogen Energy* **2012**, *37*, 12464.
 54. International Organization for Standardization. ISO 14687:2019. Hydrogen fuel quality—product specification. **2019**, <https://www.iso.org/standard/69539.html>.
 55. SAE International. SAE J2719:2020. Hydrogen fuel quality for fuel cell vehicles 2020. https://www.sae.org/standards/content/j2719_202003/.
 56. European Committee on Standardisation. EN 17124:2018. Hydrogen fuel product specification and quality assurance Proton Exchange Membrane (PEM) fuel cell applications for road vehicles 2018. <https://standards.iteh.ai/catalog/standards/cen/9388749c-d066-4255-9042-d53b710f6421/en-17124-2018>.
 57. G. Postole, A. Auroux, *Int J Hydrogen Energy* **2011**, *36*, 6817.
 58. N. Zamel, X. Li, *Prog Energy Combust Sci* **2011**, *37*, 292.
 59. J. D. Kim, P. Y. Il, K. Kobayashi, M. Nagai, M. Kunitatsu, *Solid State Ionics* **2001**, *140*, 313.
 60. N. Wagner, E. Gülzow, *J Power Sources* **2004**, *127*, 341.
 61. M. A. Rubio, A. Urquía, S. Dormido, *Int J Hydrogen Energy* **2010**, *35*, 2586.
 62. J. J. Baschuk, X. Li, *Int J Energy Res* **2001**, *25*, 695.
 63. M. C. Bétournay, G. Bonnell, E. Edwardson, D. Paktunc, A. Kaufman, A. T. Lomma, *J Power Sources* **2004**, *134*, 80.
 64. United States Environmental Protection Agency (EPA). Air Trends 2020. <https://www.epa.gov/air-trends/>.
 65. Regione Liguria. Qualità dell'aria 2021. https://servizi.regione.liguria.it/page/welcome/QUALITA_ARIA.
 66. Y. Zhao, Y. Mao, W. Zhang, Y. Tang, P. Wang, *Int J Hydrogen Energy* **2020**, *45*, 23174.
 67. F. A. De Bruijn, D. C. Papageorgopoulos, E. F. Sitters, G. J. M. Janssen, *J Power Sources* **2002**, *110*, 117.
 68. V. A. Sethuraman, J. W. Weidner, *Electrochim Acta* **2010**, *55*, 5683.

69. F. Uribe, S. Gottesfeld, T. A. Zawodzinski, *J Electrochem Soc* **2002**, *149*, A293.
70. J. J. Baschuk, X. Li, *Int J Energy Res* **2003**, *27*, 1095.
71. B. Shabani, M. Hafttananian, S. Khamani, A. Ramiar, A. A. Ranjbar, *J Power Sources* **2019**, *427*, 21.
72. A. V. Petukhov, W. Akemann, K. A. Friedrich, *Surf Sci* **1998**, *402–404*, 182.
73. Y. Zhai, K. Bethune, G. Bender, R. Rocheleau, *J Electrochem Soc* **2012**, *159*, B524.
74. W. Shi, B. Yi, M. Hou, F. Jing, H. Yu, P. Ming, *J Power Sources* **2007**, *164*, 272.
75. D. Imamura, Y. Matsuda, Y. Hashimasa, M. Akai, *ECS Trans* **2011**, *41*, 2083.
76. I. Profatlova, P.-A. Jacques, S. Escribano, *J Electrochem Soc* **2018**, *165*, F3251.
77. C. Y. Chen, C. C. Chen, S. W. Hsu, M. P. Lai, W. H. Lai, W. M. Yang, *Energy Procedia* **2012**, *29*, 64.
78. T. V. Reshetenko, K. Bethune, R. Rocheleau, *J Power Sources* **2012**, *218*, 412.
79. S. Papasavva, M. Veenstra, J. Waldecker, T. West, *Int J Hydrogen Energy* **2021**, *46*, 21136.
80. H. Li, J. Zhang, Z. Shi, D. Song, K. Fatih, S. Wu, H. Wang, J. Zhang, N. Jia, S. Wessel, R. Abouatallah, N. Joos, *J Electrochem Soc* **2007**, *154*, B609.
81. W. Shi, B. Yi, M. Hou, F. Jing, P. Ming, *J Power Sources* **2007**, *165*, 814.
82. Y. A. Gomez, A. Oyarce, G. Lindbergh, C. Lagergren, *J Electrochem Soc* **2018**, *165*, F189.
83. A. Talke, U. Misz, G. Konrad, A. Heinzl, *J Electrochem Soc* **2018**, *165*, F3111.
84. F. Jing, M. Hou, W. Shi, J. Fu, H. Yu, P. Ming, B. Yi, *J Power Sources* **2007**, *166*, 172.
85. R. Mohtadi, W. K. Lee, J. W. Van Zee, *J Power Sources* **2004**, *138*, 216.
86. T. Reshetenko, B. L. Ben, *J Power Sources* **2021**, *492*, 229657.
87. J. Zhai, M. Hou, D. Liang, Z. Shao, B. Yi, *Electrochem Commun* **2012**, *18*, 131.
88. Y. Zhai, G. Bender, S. Dorn, R. Rocheleau, *J Electrochem Soc* **2010**, *157*, B20.
89. I. Urdampilleta, F. Uribe, T. Rockward, E. L. Brosha, B. Pivovar, F. H. Garzon, *ECS Trans* **2019**, *11*, 831.
90. U. Misz, A. Talke, A. Heinzl, G. Konrad, *Fuel Cells* **2016**, *16*, 444.

How to cite this article: E. Gadducci, T. Reboli, M. Rivarolo, L. Magistri, *Fuel Cells*. **2022**, *22*, 241.
<https://doi.org/10.1002/fuce.202200062>